Building porosity for better urban ventilation in high-density cities – A computational parametric study

Chao Yuan*, Edward Ng

School of Architecture, The Chinese University of Hong Kong, Rm. 701, Wong Foo Yuan Building, Hong Kong

ABSTRACT

Shape-edged buildings impose large frictional drag on the flow in the urban boundary layer. In the subtropics, especially during hot and humid summers, compact building blocks create stagnant air that worsens outdoor urban thermal comfort. The current study adapts the $\kappa-\omega$ SST turbulence model to simulate air flow in urban areas. The accuracy of the $\kappa-\omega$ SST turbulence model in detecting air flow around a rectangular block is validated by comparing it with the data from the wind tunnel experiment. In the computational parametric study, wind speed classification is derived based on Physiological Equivalent Temperature (PET) to evaluate the effect of wind speed on outdoor thermal comfort. Numerical analysis compares the effects of different building morphology modifications on pedestrian-level natural ventilation. Critical design issues are also identified. From both the accuracy and practical points of view, the current study allows city planners and architects to improve building porosity efficiently for better pedestrian-level urban ventilation, without losing land use efficacy.

© 2011 Elsevier Ltd. All rights reserved.

1. Introduction

1.1. Background

Currently, cities are homes to more than half of the world's population and population in towns and cities will reach 4.96 billion by 2030 [1]. Urbanization improves living standards but increases the demand on natural resources at the same time [2]. High-density living in high-rate urbanization enables cities to utilize resources more efficiently by decreasing traffic cost and other energy usage [3]. However, designing high-density cities should also provide solutions to serious environmental problems caused by congested urban conditions [4].

Hong Kong, as one of the high-density cities in the world, is highly efficient in utilizing land use and public transport. Fig. 1 presents the extremely rapid and successful growth of Hong Kong in the last century. However, the high rate of urbanization in Hong Kong has largely affected low-level air flow. Optimizing urban permeability to ensure adequate natural ventilation in urban areas is a major design problem faced by city planners and architects.

High-rise compact building blocks and deep street canyons are unique urban form characteristics of Hong Kong, as shown in Fig. 2.

Stagnant air in outdoor urban spaces worsens outdoor urban thermal comfort and urban air pollution dispersion. In summer, a decrease in wind speed from 1.0 m/s to 0.3 m/s is equal to 1.9 °C temperature increase, and outdoor thermal comfort under typical summer conditions requires 1.6 m/s wind speed [5]. Wind data from an urban observatory station of Hong Kong Observatory (HKO) indicate that the mean wind speed at 20 m above the ground level in urban area, Tseung Kwan O, has decreased by about 40%, from 2.5 m/s to 1.5 m/s over the last 10 years [6]. The frequent occurrence of high concentrations of pollutants, such as NO_2 and respirable particles (RSP), in urban areas like Mong Kok and Causeway Bay has been reported by The Hong Kong Environmental Protection Department because of poor dispersion [7]. After the outbreak of the Severe Acute Respiratory Syndrome (SARS) in 2003, the Hong Kong Special Administrative Region (HKSAR) Government strived to improve the local wind environment for better urban living quality. Relevant studies, policies, and technical guidelines, such as Air Ventilation Assessment (AVA) and Sustainable Building Design (SBD) Guidelines (APP-152), have been conducted on the urban planning and design process [8].

The Hong Kong Planning Department initiated the "Feasibility study for establishment of air ventilation assessment (AVA) system" in 2003. This study was to answer the fundamental question of "*how to design and plan our city fabric for better natural air ventilation?*" [6]. The current air ventilation issues in Hong Kong were provided, and the corresponding qualitative urban design

* Corresponding author.
  E-mail address: yach@cuhk.edu.hk (C. Yuan).

Fig. 1. View of the Kowloon Peninsula and Hong Kong island in the 1900s and today. Source [48,49].

guidelines were given. The ultimate purpose of this study is to provide methodologies and guidelines to create an acceptable urban wind environment.

Unlike AVA, the SBD Guidelines (under APP-152 of Buildings Department HKSAR) are intended for building scale, which provides the quantitative requirements for three building design elements, namely, building separation, building set back, and site coverage of greenery. The SBD Guidelines aim to mitigate the negative effects of new building development on the existing surrounding wind environment and enhance the environmental quality of living spaces in Hong Kong. Without CFD simulation and wind tunnel experiment, SBD Guidelines enable architects to mitigate the undesirable effect of new buildings by modifying some simple design indexes, such as building length, distance to the adjunct streets or site boundary, width of the building gap, and size of wind permeability.

1.2. Objectives of this study

The grid plan, which dates from antiquity, is widely used in planning mega cities, such as Manhattan, Philadelphia, and Mong Kok in Hong Kong. The urban fabric of Mong Kong is presented in Fig. 3. Pursuing with the AVA and SBD Guidelines, the current study takes the urban fabric of Mong Kok as an example to examine the pedestrian-level natural ventilation performance in the context of a regular street grid.

The computational parametric study is conducted in the current study to attain two objectives. First, the study aims to evaluate the effect of rapid urbanization in the last century (Fig. 1) on natural ventilation and predict wind performance in the future. Second, it aims to derive a scientific understanding of an acceptable outdoor thermal comfort in summer in choosing appropriate design and planning strategies to efficiently improve the pedestrian-level

natural ventilation in a regular street grid while preserving land use efficacy.

2. Literature review

2.1. Layer structure of the wind environment

Wind field in the urban boundary layer is dramatically changed by urban geometry [9–12] because buildings produce greater frictional drag than other surface roughness elements in a natural environment [13]. The layer structure of the air flow above the urban areas has been widely discussed [9,14,15]. As shown in Fig. 4, Oke [9] provided the logarithmic wind profile in a neutral atmosphere, which is a semi-empirical relationship acting as a function of two aerodynamic characteristics, namely, roughness length ($z0$) and zero-plane displacement height (zd). Grimmond and Oke [11] suggested a physical phenomenon to explain the need for zd in the function. With more and more new roughness elements being added to the surface, the new roughness elements decrease the drag force of those already on the surface because of mutual sheltering. The effective height of the canopy for momentum exchange is reduced. Therefore, to validate the logarithmic wind profile formula in urban areas, a new "ground surface" (zero velocity in the wind profile) is set to $zd + z0$ [16], as shown in Fig. 4. The height of the zero velocity level is found to be about 1.5−2 m below the mean height of buildings; below this level, any wind velocity profile is possible [14].

The prediction and evaluation of air flow in the urban canopy layer (below the level of $zd + z0$) are necessary to solve several urban environmental problems, such as high heat island intensity and serious air pollution. Several studies in the last 30 years have focused on the wind environment in this layer [12], applying the following methods, scales, and objectives:

Fig. 2. High-rise compact building blocks and deep street canyons in Hong Kong. Source [50] and Google™.

Fig. 3. Urban fabric of Mong Kok: The grid plan.

a. Methods: field measurement [17], morphometric (geometric) method [15], wind tunnel experiment [18,19], and CFD simulation [20–22];
b. Scales: urban scale [23,24] and building scale [19,25];
c. Subjects: real urban morphologies [23,24] and generic building blocks [19,25].

Hussain and Lee [19] conducted a wind tunnel study on building scale, which clarifies three categories of air flow in the gap between two buildings arranged along the wind direction: isolated, wake interference, and skimming flows. This wind tunnel work is consistent with the understanding of Grimmond and Oke [11]. Blocken et al. [25] evaluated the air flow in the gap between two parallel buildings arranged across the wind direction using the commercial CFD code (Fluent 6.1.22). The study indicates that the pedestrian-level wind speed is accelerated in the passages between two parallel buildings.

The abovementioned studies focus on low-rise generic buildings blocks. In studying a real urban condition with high-rise and high-density buildings, Ng et al. [24] drew a surface roughness map to detect the pedestrian-level air paths in urban areas using the frontal area density and ground coverage ratio. Compared with this surface roughness study, which is based on the understanding from the morphometric approach, Letzel et al. [26] clarified the characteristics of air flow through complex urban geometry by conducting CFD simulations: a high-resolution parallelized Large Eddy Simulation (LES) simulation.

2.2. Outline of CFD numerical methods for neutral turbulence flows

The last 30 years have seen the remarkable rapid development of the application of CFD in environmental design. CFD has already been used not only as an environmental research tool to enlarge our predictive power but also as a design tool for urban planners and
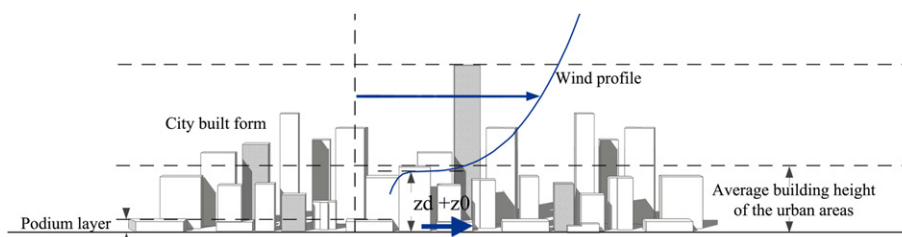

Fig. 4. Layer structure of the wind environment in the urban areas of Hong Kong. The logarithmic wind profile is presented. Below the level of $z_d + z_0$, any wind profile is possible.

designers [27]. Highly unsteady and three-dimensional turbulent flows in the atmospheric boundary can be simulated. Three methods are broadly discussed: Direct Numerical Simulation (DNS), LES, and Reynolds-averaged Navier−Stokes (RANS).

Compared with laminar flows, the fluctuations of turbulent flows are on a broad range of spatial and temporal scales [27,28]. In DNS, all spatial and temporal scales of the turbulence motions are directly computed by Navier−Stokes equations without any approximations by turbulence models [28]. Therefore, DNS is the most accurate among all of the simulation methods. However, all the length scales of turbulence should be resolved in the meshes [28]. Thus, DNS computation to simulate the flows at high Reynolds numbers becomes extremely expensive.

LES method separates the turbulence flow into large and small scales and only focuses on the "large eddy". Small eddies, such as eddies in Kolmogorov scales, are eliminated from the solution to decrease computational cost. The unresolved scales of turbulence flows are approximated by the sub filter-scale turbulence models [29,30]. Therefore, LES is less computationally costly than DNS. Currently, sufficient computer resources from parallel supercomputers enable the use of LES as a research tool, which is practical in a wide range of engineering applications to simulate high Reynolds flows, such as simulations of the neutral atmospheric boundary layer [26].

Compared with DNS and LES methods, which are time-dependent approaches, the RANS method does not directly compute any turbulence by Navier−Stokes equations but approximates the turbulence flows by decomposing solution variables in DNS and LES into the time-averaged and fluctuating components:

$$f = <f> + f' \qquad (1)$$

where f is the instantaneous value of variables, such as velocity, in the Navier−Stokes equations, $<f>$ is the mean value, and f' is the fluctuating value. The turbulence models are to approximate the effects of f'. Therefore, compared with DNS and LES, RANS is a simplified engineering approximation broadly applied as a design tool.

3. Simulation method − RANS κ−ω SST model

According to the literature review in Section 2.2, the increasing number of turbulence flows (eddies) approximated by turbulence models considerably decrease computational cost, from DNS, LES to RANS. The current study tries out the RANS method to simulate the wind velocity in the neutral condition in the computational parametric study.

3.1. RANS and turbulence model selection (κ−ω SST turbulence models)

Reynolds-averaged equations are yielded by substituting Equation (1) to the Navier−Stokes equations. The incompressible flow equations with constant density (ρ) i.e., air flow in this study, can be written as follows:

$$\text{Continuity equation}: \frac{\partial <u_i>}{\partial x_i} = 0 \qquad (2)$$

$$\text{Momentum equation}: \frac{D <u_i>}{Dt}$$
$$= -\frac{1}{\rho} \cdot \frac{\partial <P>}{\partial x_i} + \frac{\partial}{\partial x_j}\left(v \frac{\partial <u_i>}{\partial x_j} - <u_i' u_j'> \right) \qquad (3)$$

where $x_i(i = x,y,z)$ are the coordinates, u_i are the velocity vectors, t is time, v is the dynamic viscosity, and p is the pressure.

Equations (2) and (3) are similar with the Navier−Stokes equations, except that all variables in Equations (2) and (3) are time averaged, and the Reynolds stresses, $- <u_i' u_j'>$, must be approximated by turbulence models to close Equations (2) and (3).

According to the different approaches of dealing with Reynolds stresses, $- <u_i' u_j'>$, the turbulence models can be categorized into two types: a) Boussinesq Approach−turbulence viscosity (κ−ε and κ−ω turbulence models) and b) Reynolds Stress Models (RSM). The RSM turbulence model, as an anisotropic model, attempts to consider the effects of Reynolds stress by using six equations to compute the $- <u_i' u_j'>$ directly. Therefore, RSM computation is more costly than the κ−ε and κ−ω turbulence models, where ε (turbulence dissipation rate), or ω the (specific dissipate rate) is assumed isotropic. RSM is more accurate than the κ−ε realized model in flows with strong anisotropic effects (i.e., swirling flows) [31]. However, in normal flows, the accuracy of RSM is similar to the models by Boussinesq Approach [32]. More validation and cross-comparison studies are required for the application of RSM models in urban wind environment, especially in the low-wind, high-rise, and high-density urban environment.

Both turbulence viscosity and RSM models are provided by the commercial CFD code, such as PHOENICS and Fluent. The current study applies the κ−ω SST models in the computational parametric study. The κ−ω SST model is a combination of the standard κ−ω model and κ−ε model. Walls are the main source of turbulence; therefore, the accurate near-wall treatment is significant for useful turbulence models [33]. The standard κ−ω model, as a near-wall model, is more accurate than the κ−ε models in the near-wall layers [34]. However, the standard κ−ω model cannot replace κ−ε models in the simulation of the outer part of the near-wall region [34]. The κ−ω SST model uses the standard κ−ω model for the inner part and gradually changes to the κ−ε model for the outer part [33,34].

3.2. Validation

Cross-comparisons of wind data from RANS (κ−ε models), DES, LES, and the wind tunnel experiments were conducted by a working group from the Architectural Institute of Japan (AIJ) to calibrate the CFD simulation results [20,35]. The current study validates the accuracy of the SST κ−ω model by comparing the simulation results with the wind tunnel data from AIJ.

Menter and Kuntz [34] compared the simulation results obtained from κ−ω SST and DES SST models. The data for comparison were a set of vertical mean wind velocity profiles across a single cubic block. The comparison result suggests that κ−ω SST, as well as the DES SST model, can predict air flow near the building, but it fails to reproduce the recovery downstream in the separation zone, which is far from the building [34]. The current study mainly focuses on the pedestrian-level wind environment. Therefore, both the pedestrian-level wind speed distribution and vertical wind velocity profiles are compared with the data from the wind tunnel experiment.

3.2.1. Computational modeling

The accuracy of the simulation results significantly depends on the appropriate computational modeling, such as the domain size, grid size, and grid discrepancy. Therefore, the CFD simulation modeling for this validation experiment and the following parametric study comply with the AIJ guidelines for the urban pedestrian wind environment. AIJ guidelines are based on a number of cross-comparisons among CFD, wind tunnel experiments, and field
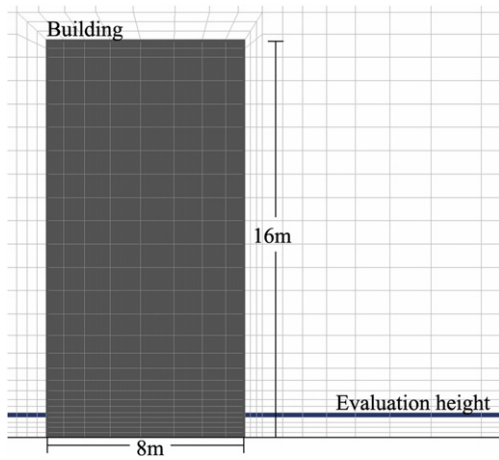
Fig. 5. Cross-section of the buildings and grids. The maximum grid size ratio is set to 1.2 and four mesh layers are arranged below the evaluation height.

measurements. By contrast, another popular guideline, COST recommendations, is based on the literature review [20].

The computational domain size for the validation experiment is 500 m × 500 m × 60 m (W × L × H). The domain is divided into 139,170 grid points. As shown in Fig. 5, adaptive meshing method is applied to predict accurately the flows at the areas of interest and use the computational resources efficiently. Fig. 5 shows that the finer scale grids are arranged at the areas around the building and close to the ground. To comply with the AIJ guidelines, four layers (layer height: 0.5 m) are arranged below the evaluation height (2.25 m above the ground). The maximum grid size ratio is set to 1.2, as shown in Fig. 5.

3.2.2. Boundary condition and validation results

The inlet mean wind speed profile is set to

$$U_{(h)} = U_{met} \cdot \left(\frac{h}{d_{met}}\right)^a \tag{4}$$

where a is the surface roughness factor ($a = 0.2$), U_{met} is the wind speed at the top of the domain ($U_{met} = 6.751$ m/s), d_{met} is the domain thickness ($d_{met} = 60$ m) and h is the height. To compare with data from the wind tunnel experiment, the inlet wind profile in CFD simulation is set similarly as possible to the one from the wind tunnel experiment, as shown in Fig. 6. The outlet wind profile is set same as the inlet wind profile.

The contour of wind speed at 2.25 m above the ground is presented in Fig. 6. Fig. 7 shows the position of the test points and the cross-comparing result. The linear regression analysis result ($R^2 = 0.853$) suggests that the $\kappa-\omega$ SST model can predict accurately the pedestrian-level air flow caused by shape-edged buildings. To further validate the simulation results, the vertical profiles of the mean wind velocities from CFD simulation and wind tunnel experiment at position 1 and position 2 (Fig. 7) are also presented in Fig. 8. The results are consistent with the experiment results conducted by Menter and Kuntz [34] and well compliment and validate the accuracy of the simulation. However, it should be noted that, when the wind velocity is very low, the deviations between wind tunnel data and the simulation results are larger than the standard deviation.

4. Study method: parametric study

Compared with applied studies focusing on wind performance in real urban morphologies [23,36,37], the current study uses the parametric approach to obtain the natural ventilation performance with generic building configurations. In the parametric study, cross-comparing the effects of different design issues is easier by observing changes in natural ventilation performance in different testing scenarios, thus identifying the critical design issues. Three groups, comprising 27 testing scenarios, are set up in three input wind directions and are simulated by the $\kappa-\omega$ SST model. Each testing scenario uses a building model matrix. The building model design, computational modeling of the testing scenario, and boundary conditions for CFD simulation are introduced in this section.
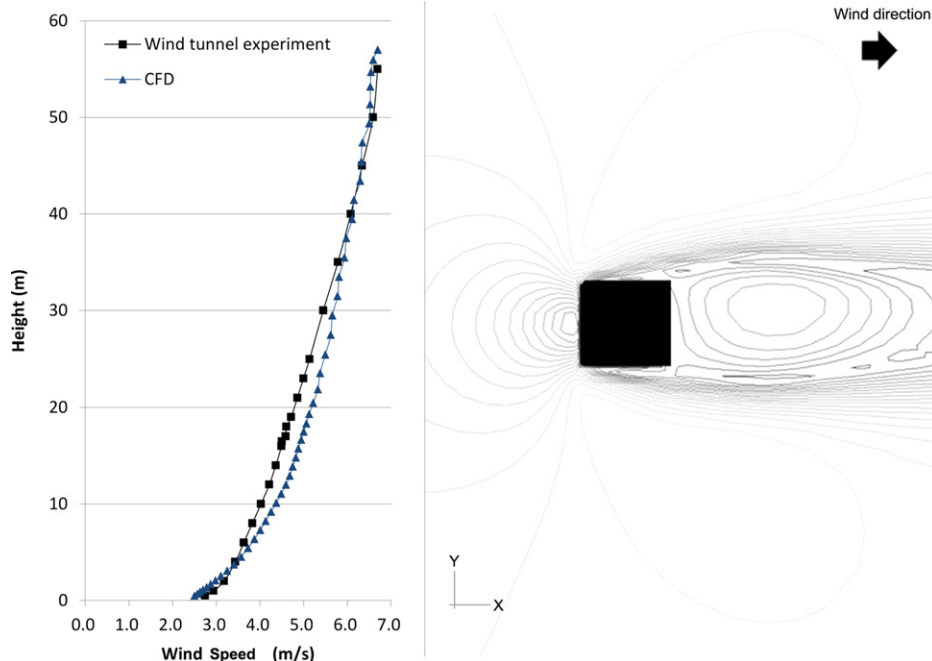

Fig. 6. Inlet mean wind speed profiles in the CFD simulation and wind tunnel experiment, and the simulation result (the contour of wind speed at 2.25 m above the ground).
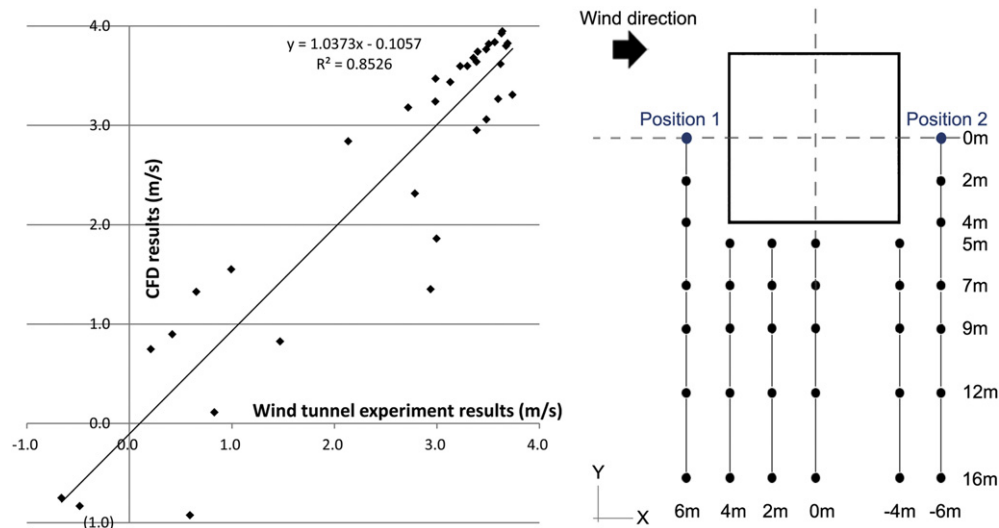
Fig. 7. Test points and the linear correlation of wind speeds from the CFD simulation and wind tunnel experiment (significant level: 0.95).

4.1. Building models for the parametric study

Nine building models are designed to test the effects of different building morphologies on natural ventilation performance. The summary of these models is presented in Fig. 9. The site area remains the same at 200 m × 100 m.

To evaluate the effect of urbanization on the urban natural ventilation and predict future conditions, three models (i.e. Cases 1903, 1, and 2) are designed based on the urban morphologies of the past, present, and future Mong Kok area in Hong Kong. The downtown area of Mong Kok has significantly changed over time. Compared with the Mong Kok of 1903, the present Mong Kok is extremely high density; the population density is mean 130,000 per km^2 [38]. Furthermore, given the present planning trend, the future population density of this downtown area will be much higher than the current density. Case 1903 is Mong Kok of the past characterized by three or four-floor buildings with a sloping roof. In the simplified parametric model, the sloping roof is replaced by a flat floor and 20 m building height. Case 1 is the present Mong Kok in which the height of buildings and podiums is on average 45 m and 15 m, respectively [24]. The site area is not fully occupied, and a narrow gap exists. Case 2 is Mong Kok in the future in which the height of buildings is on average estimated to increase to 90 m. Moreover, the site area will be fully occupied in response to the increasing need for the land use.

To mitigate the negative wall effects caused by the alignment of long and tall buildings, various modification strategies are included, such as setting back buildings, separating the long buildings, stepping the podium, opening the permeability of towers and podiums, and creating a building void between towers and podiums. The efficiency of these modifications are tested together or individually by establishing six corresponding models (i.e. Cases 3—6a and b, and 7), as shown in Fig. 9. In Cases 3—7, the building volumes are similar to the one in Case 2 to keep the land use density constant.

Case 3 is similar to Case 2, except that the building is set back 15 m along the street in Case 3. It is opined that setting back buildings is relatively easy be applied in urban planning. Building separations along the prevailing wind direction are applied in Case 4. The decreased land use efficiency resulting from the building separations is compensated by higher towers (123 m). Case 5 is the combination of Cases 3 and 4. The stepped podium and building

void in Case 6 are popular design strategies in Hong Kong, which are favorable for natural outdoor ventilation and greening. Air passages in high and wide buildings are applied in Case 7. This strategy is currently widely used in Hong Kong to mitigate the undesirable effects on the leeward wind environment.

4.2. Computational modeling

The computational modeling for the urban scale is used in the current study. Several parametric studies for wind evaluation and prediction are in the building scale, focusing on the air flow around only one or two simple and generic buildings [22,25,39]. However, the turbulence kinetic energy produced by the urban context is difficult to be reproduced in the inlet boundary condition. The testing scenario modeled in the urban scale can approximately include the effect of urban context on air flow to evaluate and predict more accurately the natural ventilation performance in the area of interest.

In the current study, 27 testing scenarios are simulated in the neutral condition by the κ—ω SST model in three wind directions (0°, 45°, and 90°). As shown in Fig. 10, each testing scenario is made up of a corresponding model array (6 × 10) and two rows of surrounding randomized buildings. The same regular street grid is applied in all model arrays; the width of the street canyon is 20 m. To consider the effects of the urban context, only the wind data measured at the target area (Fig. 10) are used for numerical analysis.

The computational domain size is 3.2 km × 3 km × 0.45 km (W × L × H), as shown in Fig. 10. The grid point numbers are about 5.0—6.8 million on a case-by-case basis. Similar to the meshes in the validation study, the finer meshes are arranged at the areas around the buildings and close to the ground. To comply with the AIJ guideline, the maximum of the grid size ratio is set to 1.2, and the three grid layers (layer height: 1 m) are arranged below the evaluation level, indicating that the wind field at 3.5 m above the ground is analyzed.

To set the inlet boundary condition, especially for the Mong Kok area, by Equation (4), the site-specific annual wind rose data at a 450 m height are obtained from the fifth-generation NCAR/PSU meso-scale model (MM5) [40]. As shown in Fig. 11, wind from the east and northeast sectors have the higher probability of occurrence, with wind from the northeast being the highest. Therefore, one of the input wind directions in the simulation is set to 90° as
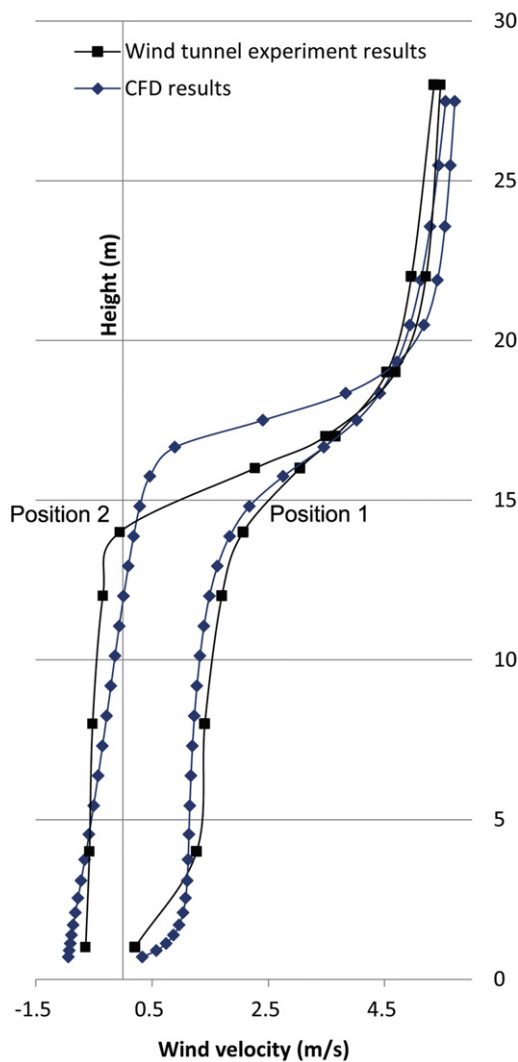
Fig. 8. The vertical profiles of the mean wind velocities from the CFD simulation and wind tunnel experiment. Locations of the vertical lines: Position 1 (windward) and 2 (leeward), as shown in Fig. 7.

the prevailing wind direction. Simulations in the input wind directions of 0° and 45° (Fig. 10) are also included to describe comprehensively the natural ventilation performance in different wind directions. Wind speed at the top of the domain is set to U_{met} = 11 m/s. It is the mean prevailing wind speed at a 450 m height in the summer. Owing to the high urban surface roughness, surface roughness factor (a) is set to 0.35 in this computational parametric study. The outlet wind profile is set same as the inlet wind profile.

5. Result analysis

5.1. Wind speed classification

For the performance-based analysis of the simulation results, a wind speed classification based on outdoor thermal comfort is derived. The earliest study on wind speed classification is by Beaufort (cited in [41]). Murakami and Deguchi [42] provided speed criteria for wind load effects on pedestrians by conducting a large wind tunnel test and field experiments. Unlike the above-mentioned classifications in which wind is a kind of "nuisance", the

current study considers wind as a benefit. Therefore, this classification is based on the outdoor thermal comfort and not on the wind force on pedestrians or buildings. Ng et al. [43] conducted a survey to obtain the pedestrian-level wind speed threshold values, especially for outdoor thermal comfort in Hong Kong, using physiological equivalent temperature (PET) [44]. In a typical summer day when air temperature is 27.9 °C and relative humidity is about 80%, wind speed of 0.6–1.3 m/s is required to achieve neutral thermal sensation (neutral PET: 28.1 °C). In another survey on thermal comfort in Hong Kong [5], the wind speed settings with and without wind break are 0.3 m and 1.0 m, respectively, which is equal a 1.9 °C air temperature difference.

Therefore, based on the literature review, the classification of the pedestrian-level wind speed (u) is assigned as follows: Class 1: u <0.3 m/s; Class 2: 0.6 m/s >u ≥ 0.3 m/s; Class 3: 1.0 m/s >u ≥ 0.6 m/s; Class 4: 1.3 m/s >u ≥ 1.0 m/s and Class 5: u ≥1.3 m/s. These classifications denote "stagnant," "poor," "low," "satisfactory," and "good" pedestrian-level natural ventilations in street canyons, respectively.

5.2. Comparison of the natural ventilation performances in three input wind directions

The parts of the contours of mean wind speed in Case 1 are presented in Figs. 12 and 13. The randomized cubic buildings prevent input air flow from directly entering into the gaps between two parallel buildings, enabling a more similar simulation results with the wind environment in real urban areas. As shown in Fig. 12, the accelerated wind speed is found at street canyons along with the wind direction. However, other than these areas, wind speed is significantly decelerated, especially in deep street canyons across the wind direction. When the input wind direction is changed from 90° to 45°, air flow can enter into the streets from both directions (Fig. 13). Therefore, areas with stagnant air are decreased. In the input wind direction of 0°, as shown in Fig. 13, air flow can penetrate more deeply into the streets than those in the prevailing wind direction (90°). The wind environments in three input wind directions are consistent with the statement in the AVA study: "*An array of main streets, wide main avenues and/or breezeways should be aligned in parallel, or up to 30 degrees to the prevailing wind direction, in order to maximize the penetration of prevailing wind through the district.*" [6]

5.3. Comparison of the urban natural ventilation performances of nine building morphologies

About 300 wind speed data in every test scenario are measured at the centerlines of four streets in the target area to evaluate natural ventilation performances numerically in different building morphologies (Fig. 10). Based on wind speed classification, wind data are organized using the relative frequency of the wind speed distribution to evaluate the natural ventilation performances in the target area. Cross comparison of the natural ventilation performances in the input wind direction of 90° (prevailing wind direction) is presented in Figs. 14 and 15 and in Table 1.

Fig. 14 shows the evaluation of the natural ventilation performances of the past, present, and future Mong Kok. The lowest relative frequency (2.29%) of the area with very poor natural ventilation (Class 1: u <0.3 m/s) is found in Case 1903. Case 1 analysis suggests that natural ventilation performance in the present urban form (Case 1) has worsened to 25.67% in Class 1 and 43.67% in Class 2 because of rapid urbanization in the Mong Kok area in the last century. Case 2 analysis suggests that the relative frequency of the area with very poor air ventilation in the future urban form may reach 44%.
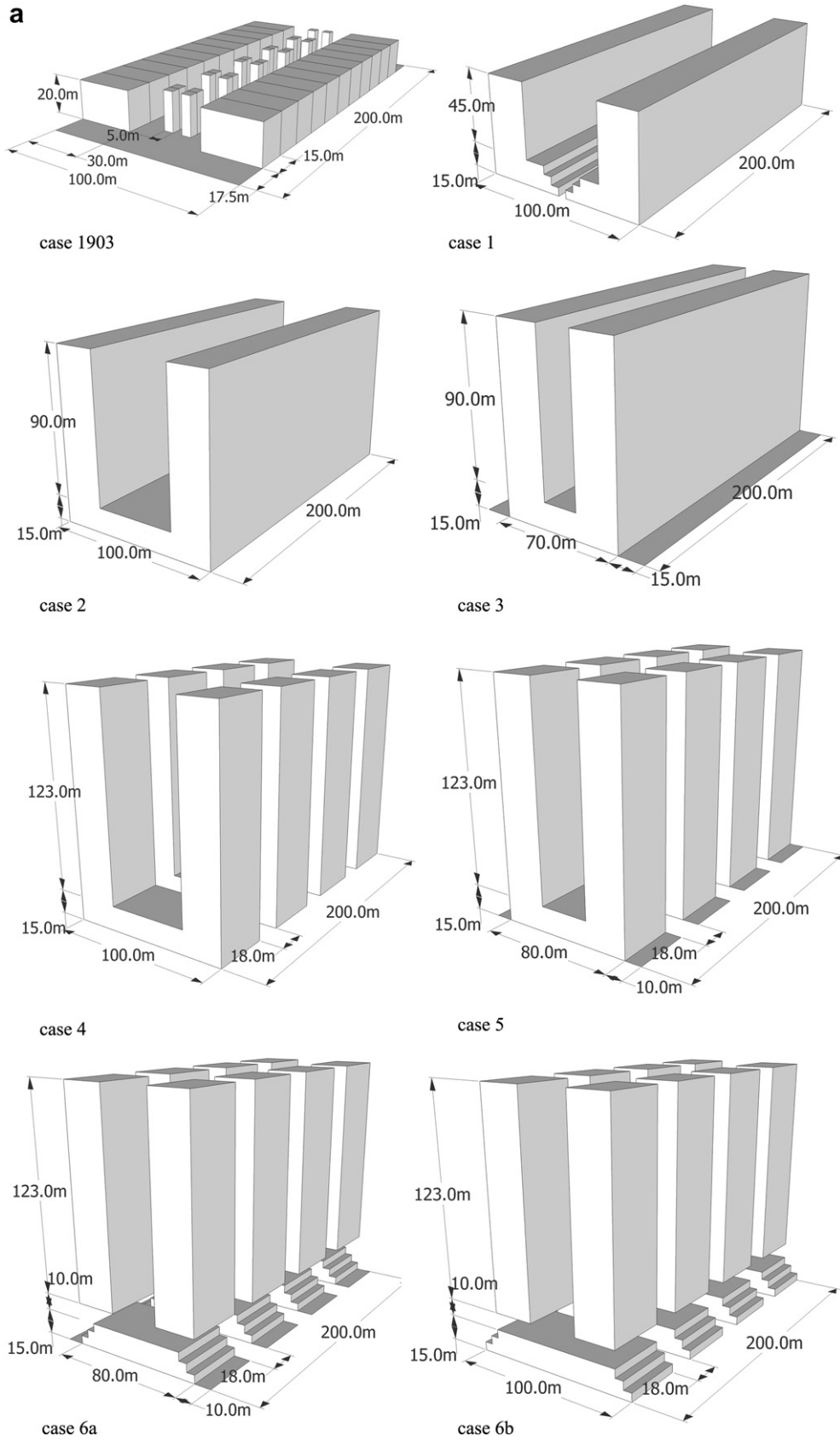
a

case 1903

case 1

case 2

case 3

case 4

case 5

case 6a

case 6b

Fig. 9. Summary of nine testing models which are designed to test the effects of different building morphologies on natural ventilation performance.
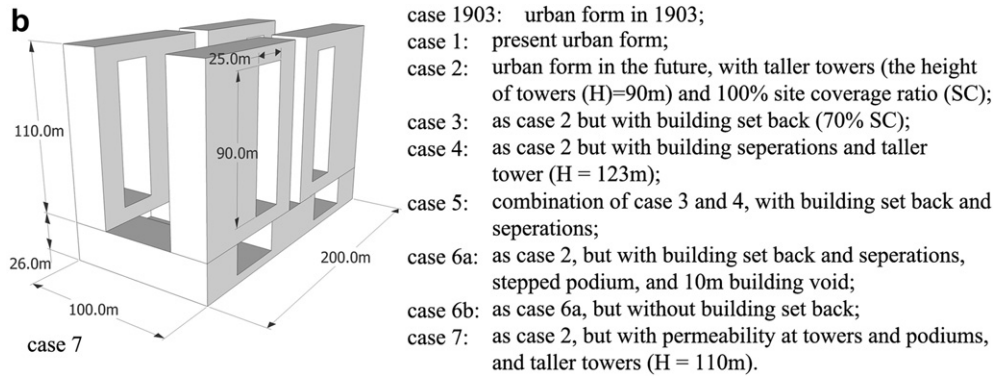
case 1903: urban form in 1903;
case 1: present urban form;
case 2: urban form in the future, with taller towers (the height of towers (H)=90m) and 100% site coverage ratio (SC);
case 3: as case 2 but with building set back (70% SC);
case 4: as case 2 but with building seperations and taller tower (H = 123m);
case 5: combination of case 3 and 4, with building set back and seperations;
case 6a: as case 2, but with building set back and seperations, stepped podium, and 10m building void;
case 6b: as case 6a, but without building set back;
case 7: as case 2, but with permeability at towers and podiums, and taller towers (H = 110m).

Fig. 9. (*continued*).

Fig. 15 presents the effects of the design issues on the urban natural ventilation performance of Cases 3–7. For comparison, the Cases 1 and 2 are also included in Fig. 15. Building setbacks (Case 3) and building separations (Case 4) are helpful in improving pedestrian-level natural ventilation. Compared with that of Case 2, the relative frequency of Class 1 in Case 3 decreased to 22.02% and 24.12% in Case 4. However, wind performances in Cases 3 and 4 are still not good enough, resembling the condition in Case 1, which represents the current urban wind environment. Both building setbacks and separations are adapted in Case 5. The relative frequency of Class 1 is decreased further to 13.06%.

Stepped podiums and 10 m building voids are applied in Cases 6a and 6b. The relative frequency of Class 1 in Case 6a is 9.83% and 2.60% in Case 6b. Results indicate good natural ventilation performance close to Case 1903, even when land use density in Case 6 is higher than that in Case 1903. Air passages in the tower and podium is applied in Case 7. However, the relative frequency in Class 1 remains very high at 44.78%.

Two similar analyses are conducted using the wind speed data in the input wind direction of 0° and 45°. First, as shown in Figs. 16 and 17, the relative frequencies of Class 5 $u \geq 1.3$ m/s are much higher than that shown in Fig. 15. The findings validate that the change in street grid direction is helpful in improving natural ventilation performance. Second, the sensitivity of the natural ventilation performance to the changes in building morphologies is low, especially in the 45° input wind direction. Low sensitivity is attributed to the modification strategies designed according to the prevailing wind direction (90°).

5.4. Comparison of the vertical profiles of the mean wind velocity

To describe the air flow in street canyons further and explain the analysis results stated in Section 5.3, the vertical profiles of the mean wind velocity are measured at a point on the centerline of the street across the prevailing wind direction, as presented in Fig. 18.

Fig. 18a shows profiles from 400 m to 0 m, indicating that building height significantly affects wind profiles, especially at zd + z0 values. The height of zero velocity in the wind profiles is close and is slightly lower than the mean height of buildings. The result is consistent with that of Oke [16] and Lawson [14].

Profiles from 50 m to 0 m are enlarged in Fig. 18b to show air flow that are close to the ground. Analysis results indicate that the wind environment at the pedestrian level is not affected by building height but is significantly influenced by building morphology in the podium layer. The results agree with the frontal area density study in the urban scale by Ng et al. [24].

6. Discussion

Based on the result analysis in Section 5, a number of understandings that are significant to urban planning and design can be stated as following:

1) Street grid orientation in grid planning is a significant parameter in urban natural ventilation performance. Main streets should be arranged along the prevailing wind direction. The efficiency of the design issues also depends on the prevailing wind direction, as demonstrated in the results in Section 5.3.
2) The mean building height decides the z0 + zd value in high-density urban areas. However, to pedestrians, urban ventilation performance mostly depends on the pedestrian-level building porosity.
3) On the whole, decreasing the site coverage ratio helps increase the pedestrian-level natural ventilation performance. Comparison among Cases 3–5 provides a more detailed understanding. Wind profiles in Cases 3 and 4 suggest that, in
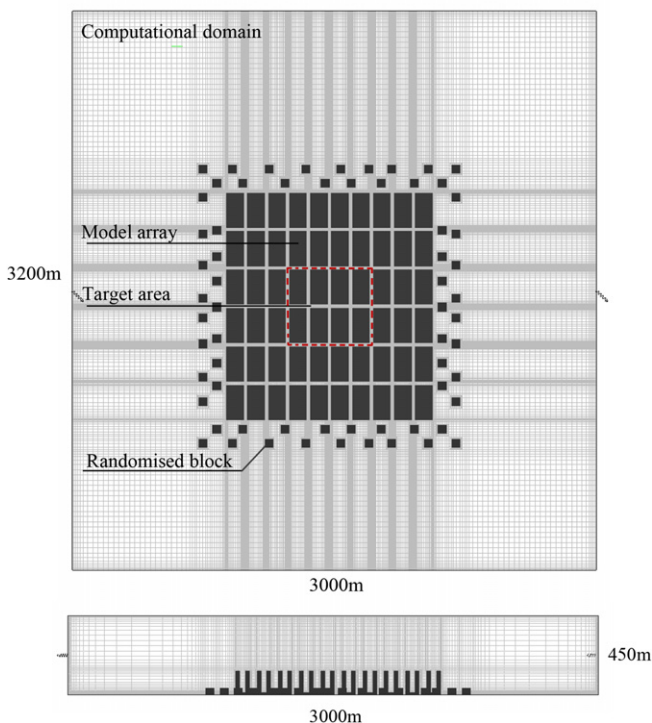

Fig. 10. Computational domain and grids for the parametric study. The model array, randomized block, and the target area are presented.
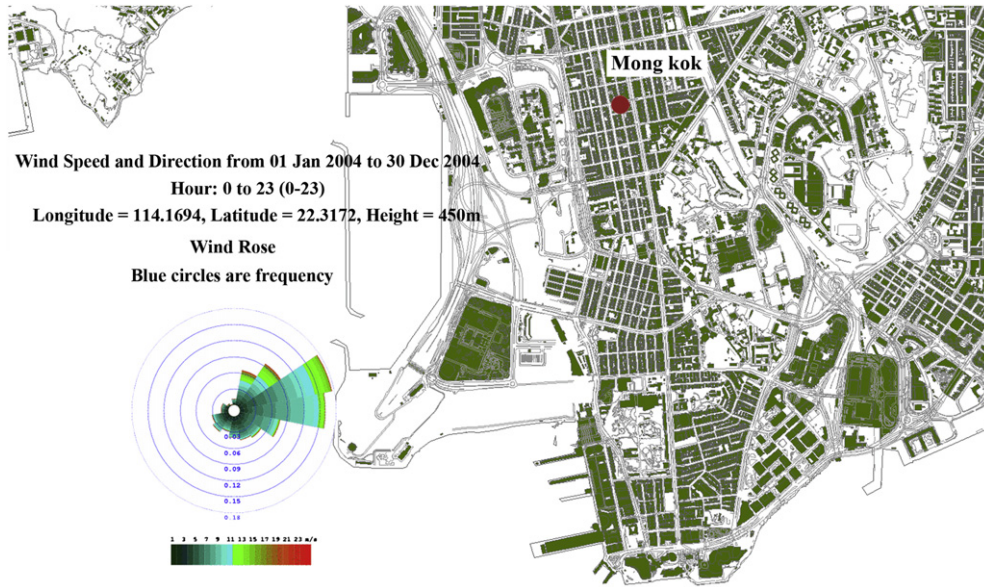
Fig. 11. Site-specific annual wind rose of Mong Kok.

high-density urban areas, building setbacks along the street across the prevailing wind direction (Case 3) are less useful than building separations along the prevailing wind direction (Case 4). On the other hand, the Case 5 (Fig. 18b) profile suggests that, if building separation is incorporated with building setback, the pedestrian-level wind speed on the leeward outdoor space can be further improved.

4) Wind permeability in the podium layer is very useful in leading air flow to deep street canyons. In Case 6, the building void between towers and podiums significantly accelerates turbulent flows in the podium layer, and the stepped podiums lead air flow to the pedestrian level. Air flow across the building void (10 m) are numerically presented as red lines in Fig. 18b. The mean wind speed on the leeward outdoor space can be improved to approach the condition in 1903.

5) Air passages should be arranged as close as possible to the ground level. Poor wind performance in Case 7 indicate that wind permeability in towers does not improve the pedestrian-level wind environment. On the other hand, compared with the profiles of case 6, it is known that the wind passage in the podium layer should incorporate the stepped podium to benefit the pedestrian-level wind environment, or the openings on the facade should be opened from the ground.

6) Building setback, separation, and building permeability are helpful in improving the pedestrian-level wind environment. However, the levels of efficiency of these strategies differ. Natural ventilation performance in urban area results from the integral effects of buildings, therefore, considering the urban area as a whole is important. As such, air paths in the areas can be efficiently established and organized by applying different
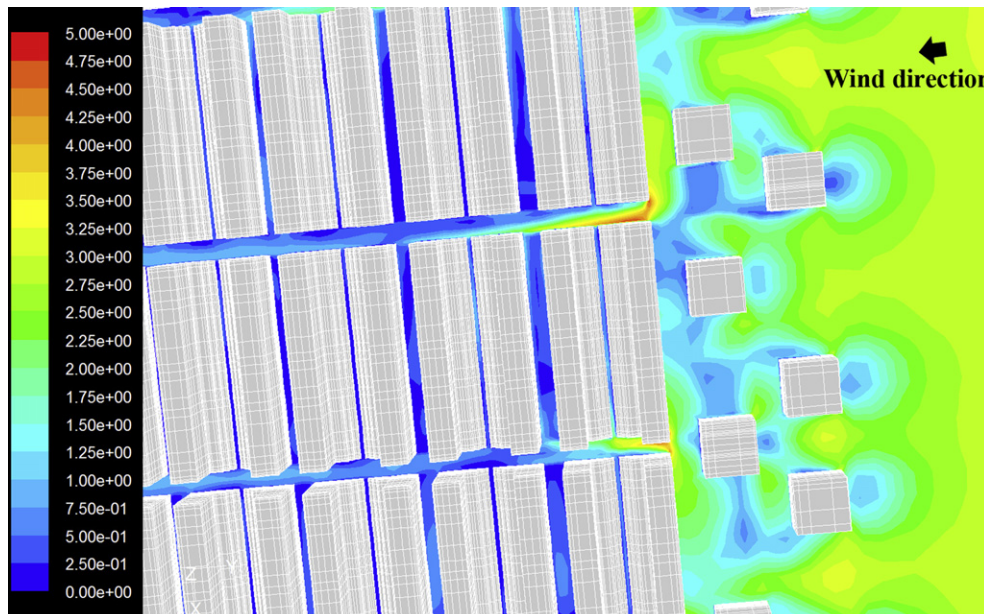

Fig. 12. Contour of wind speed in the wind direction of 90° (prevailing wind direction) at 3.5 m above the ground (Case 1).
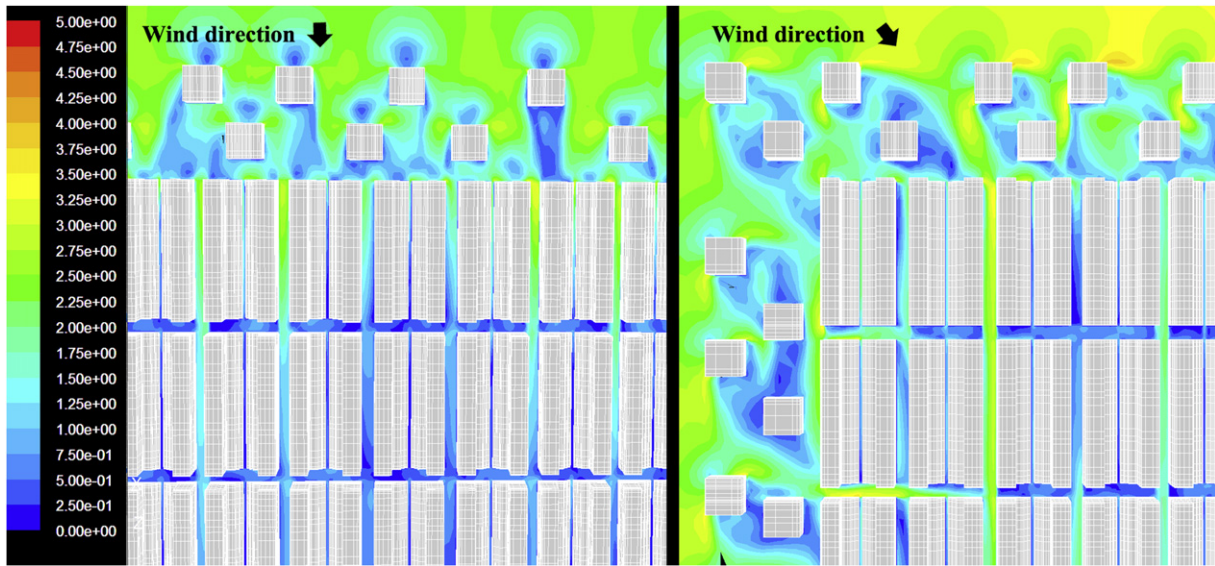
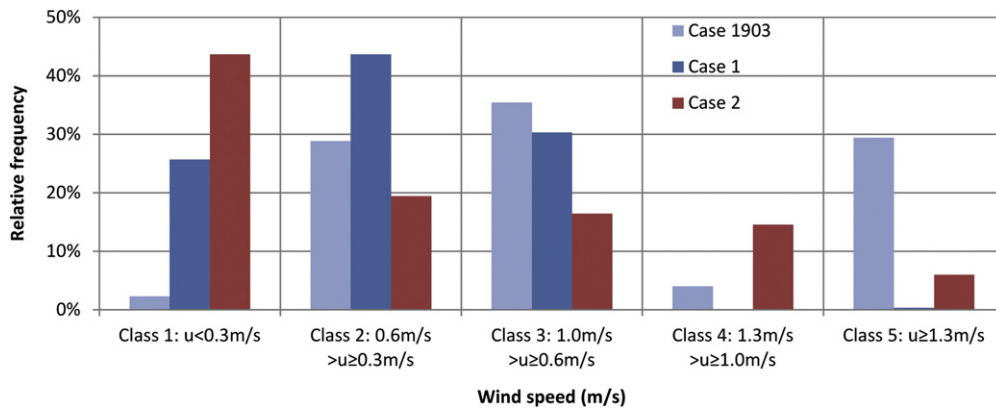**Fig. 13.** Contours of wind speed in the wind direction of 0° and 45° at 3.5 m above the ground (Case 1).

Fig. 14. Relative frequencies of pedestrian-level mean wind speed in Cases 1903, 1, and 2 (input wind direction: 90°).
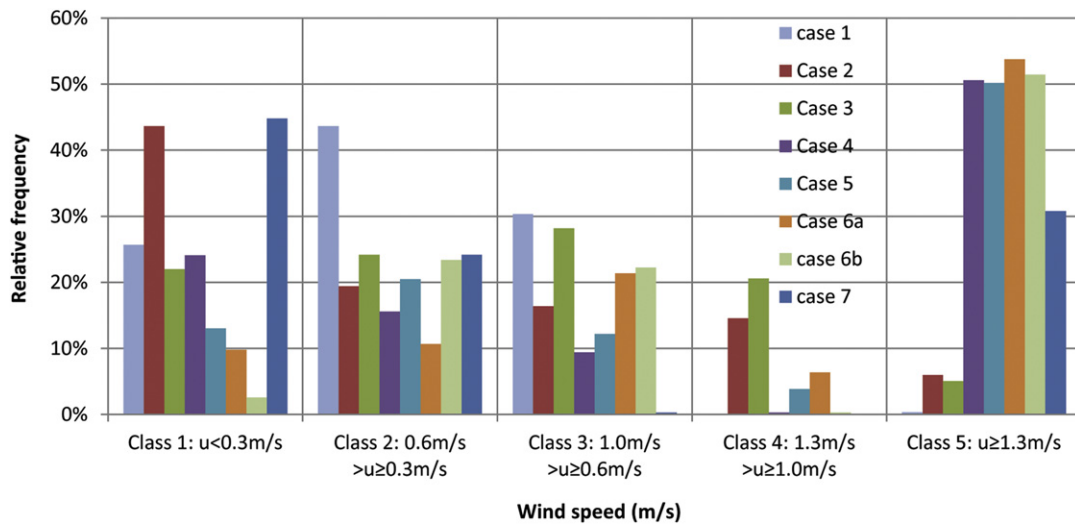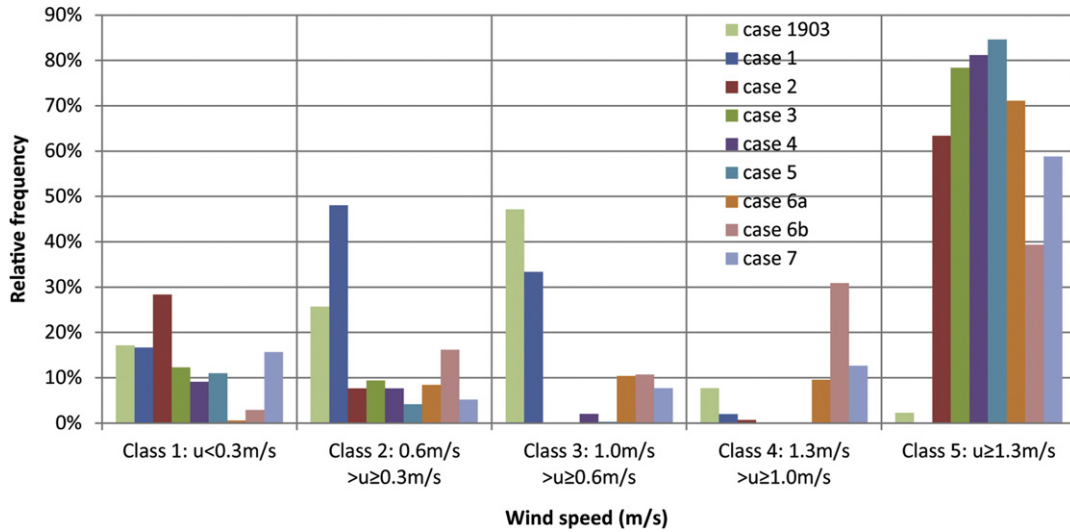

Fig. 15. Relative frequencies of the pedestrian-level wind speed in Cases 1, 2, 3, 4, 5, 6a, 6b, and 7 (input wind direction: 90°).

Table 1
Summary of the relative frequencies of pedestrian-level wind speed in nine testing models (input wind direction: 90°).

|	$u < 0.3$ m/s stagnant	0.6 m/s $> u \geq 0.3$ m/s poor	1.0 m/s $> u \geq 0.6$ m/s low	1.3 m/s $> u \geq 1.0$ m/s satisfactory	$u \geq 1.3$ m/s good
Case 1903	2.29%	28.86%	35.43%	4.00%	29.43%
Case 1	25.67%	43.67%	30.33%	0.00%	0.33%
Case 2	43.66%	19.40%	16.42%	14.55%	5.97%
Case 3	22.02%	24.19%	28.16%	20.58%	5.05%
Case 4	24.12%	15.59%	9.41%	0.29%	50.59%
Case 5	13.06%	20.47%	12.17%	3.86%	50.45%
Case 6a	9.83%	10.69%	21.39%	4.34%	53.76%
Case 6b	2.60%	23.41%	22.25%	0.29%	51.45%
Case 7	44.78%	24.18%	0.27%	0.00%	30.77%

Fig. 16. Relative frequencies of the pedestrian-level wind speed in Cases 1903, 1, 2, 3, 4, 5, 6a, 6b, and 7 (input wind direction: 0°).
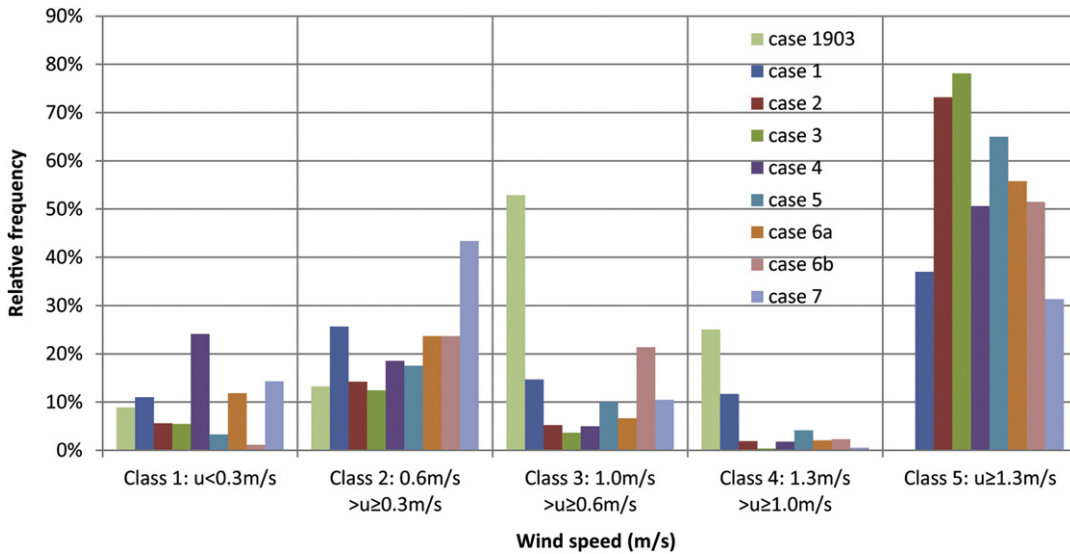
Fig. 17. Relative frequencies of the pedestrian-level wind speed in Case 1903, 1, 2, 3, 4, 5, 6a, 6b, and 7 (input wind direction: 45°).

strategies to improve building porosity. Combining several strategies (urban planning + building design) is recommended because it is usually more efficient than any single strategy. Planners and architects should choose appropriate strategies based on the actual design requirements and insights from this section.

7) The current study gives some scientific insights into the urban ventilation section of the Hong Kong Planning Standards and Guidelines (HKPSG) [45], as it stresses the importance to design into the urban plan breezeways and air path with non-building areas and building setbacks from streets. Aligning of the streets properly and leaving sufficient open spaces that can be
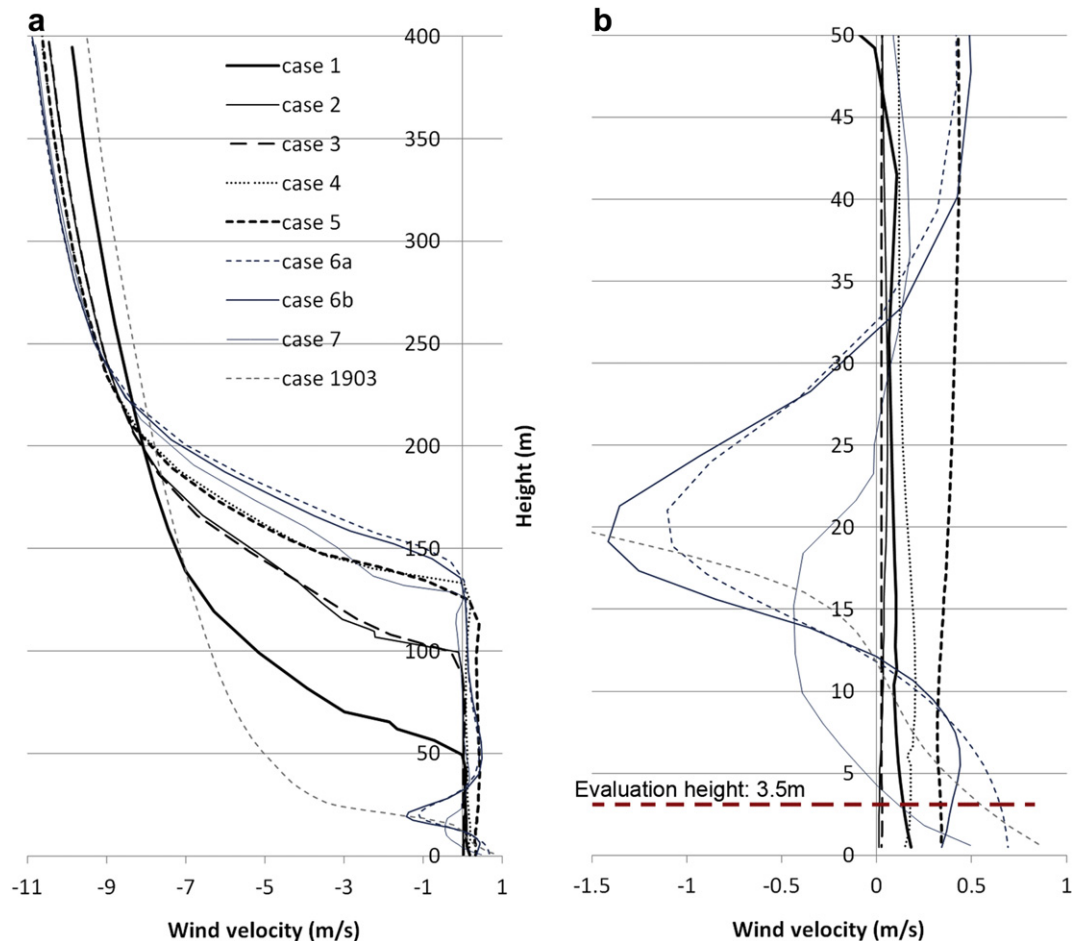
Fig. 18. Mean wind velocity profiles measured at the centerline of the street canyon across the wind direction. Profiles from 50 m to 0 m are enlarged to show air flow close to the ground.

interlinked are equally important, as well as complimenting the urban planning efforts with building level designs. Building gaps, separations, and porosity close to the pedestrian levels are extremely useful in improving air space for urban air ventilation circulation.

8) Increasing urban density has gained attention in recent world-wide discussions. Traditional wisdom attributes the decline of urban air ventilation to increasing urban density because of high urban frontal area density (FAD). This understanding is generally correct, and balancing the need to reduce land resource demand with designing more compact cities is also useful. The current study suggests that more insights should be gained to fine tune and design urban morphologies and building forms that "optimize" urban air ventilation. The optimization process can consider further the bio-meteorological needs of air ventilation in different climatic zones [5].

9) Evidence-based decision making is important, especially for market or policy transformation [46,47]. This understanding is only possible with scientific and parametric studies that examine the sensitivity and performance of various design and planning options. The parameters should be defined carefully and practically to arrive at "realistic" results.

7. Conclusion

In the current study, a computational parametric approach is presented to evaluate the effects of the different urban

morphologies on the pedestrian-level natural ventilation environment through CFD simulation. Based on the literature review, different simulation methods and turbulence models are compared. The $\kappa-\omega$ SST turbulence model is applied in this study. Results of the comparison between CFD simulation results and wind tunnel data suggest that the $\kappa-\omega$ SST turbulence model is accurate enough to simulate the turbulent flows caused by shape-edged buildings. Unlike the wind field studies in real urban areas, the current study designs a number of parametric models to test the different modification effects on pedestrian-level air flow in street canyons. Compared with other parametric studies in which only one or two buildings are included, this study employs computational modeling in the urban scale to include the effects of the urban context. This study derives a wind speed classification based on the outdoor thermal comfort, as well as uses the relative frequency of the pedestrian-level wind speed and the vertical profiles of the mean wind velocity to evaluate the natural ventilation performance in street canyons. Cross-comparison results suggest that the sensitivity of the wind performance is not same to different modifications of building morphology. Relevant planning and design strategies are provided based on the findings of this study.

8. Limitations and further study

The current study is limited by the computational parametric study, which only considers the wind environment in the urban context of a regular street grid. Other determinants, such as

building disposition and various building heights, are expected to reveal more insights in future works. More advanced simulation methods are also expected for a more accurate CFD simulation, especially for very low-wind speeds.

Acknowledgment

References

[1] Population division of the Department of Economic and Social Affairs of the United Nations Secretariat. New York: United Nations: World Urbanization Prospects: The 2007 Revision; 2011.
[2] Hong Kong ecological footprint report 2010 – Paths to a sustainable future. World Wildlife Fund. Available at: http://www.footprintnetwork.org/images/uploads/HK_EFR_2010_EN.pdf; 2010.
[3] Betanzo M. Pros and cons of high density urban environments. Build:39–40. Available at: http://www.branz.co.nz/cms_show_download.php?id=19e77a3d86f137b83b523c7057da8b00fae76c41; 2007.
[4] Ng E. Designing high-density cities. London Sterling, VA: Earthscan; 2009.
[5] Cheng V, Ng E, Chan C, Givoni B. Outdoor thermal comfort study in a subtropical climate: a longitudinal study based in Hong Kong. Int J Biometeorol; 2011. doi:10.1007/200484-010-0396-z.
[6] Feasibility study for establishment of air ventilation assessment system, final report, the government of the Hong Kong special administrative region. Hong Kong planning Department (HKPD). Available at: http://www.pland.gov.hk/pland_en/p_study/comp_s/avas/papers&reports/final_report.pdf; 2005.
[7] Yim SHL, Fung JCH, Lau AKH, Kot SC. Air ventilation impacts of the "wall effect" resulting from the alignment of high-rise buildings. Atomos Environ 2009;43(32):4982–94.
[8] Ng E. Policies and technical guidelines for urban planning of high density cities – Air ventilation assessment (AVA) of Hong Kong. Build Environ 2009; 44:1478–88.
[9] Oke TR. Boundary layer climates. 2nd ed. USA: Methuen, Inc.; 1987.
[10] Givoni B. Climate considerations building and urban design. USA: Wiley & Sons; 1998.
[11] Grimmond CSB, Oke TR. Aerodynamic properties of urban areas derived from analysis of surface form. J Applied Meteorol 1999;38:1262–92.
[12] Arnfield AJ. Two decades of urban climate research: a review of turbulence exchanges of energy and water, and the urban heat island. Int J Climatol 2003; 23(1):1–26.
[13] Taylor PA. Turbulent wakes in the atmospheric boundary layer. In: Steffen WL, Denmead E OT, editors. Flow and transport in the natural environment: advances and applications. Springer-Verlag; 1988. p. 270–92.
[14] Lawson T. Building aerodynamics. London: Imperical College Press; 2001.
[15] Bottema M. Roughness parameters over regular rough surfaces: experimental requirements and model validation. J Wind Eng 1996;64:249–65.
[16] Oke TR. Initial guidance to obtain representative meteorological observations at urban sites report no.: instruments and observing methods report no. 81 World Meteorological Organization. Available at: http://www.wmo.int/pages/prog/www/IMOP/publications/IOM-81/IOM-81-UrbanMetObs.pdf; 2006.
[17] Oke TR. Sitting and exposure of meteorological instruments at urban sites. 27th NATO/CCMS International Technical Meeting on Air Pollution Modelling and its Application, 25–29 October, Banff; 2004.
[18] Klein-Kastner P, Fedorovich E, Rotach MW. A wind tunnel study of organised and turbulent air motions in urban street canyons. J Wind Eng Ind Aerod 2001;89:849–61.
[19] Hussain M, Lee BE. A wind tunnel study of the mean pressure forces acting on large groups of low-rise buildings. J Wind Eng Ind Aerod 1980;6:207–25.
[20] Tominaga Y, Mochida A, Yoshie HK, Nozu T, Yoshikawa M, Shirasawa T. AIJ guidelines for practical applications of CFD to pedestrian wind environment around buildings. J Wind Eng Ind Aerod 2008;96:1749–61.
[21] Frank J. Recommendations of the COST action C14 on the use of CFD in predicting pedestrian wind environment. J Wind Eng 2006;108:529–32.
[22] Stathopoulos T, Storms R. Wind environmental conditions in passages between buildings. J Wind Eng Ind Aerod 1986;95:941–62.
[23] Mochida A, Murakami S, Ojima T, Kim S, Ooka R, Sugiyama H. CFD analysis of mesoscale climate in the Greater Tokyo area. J Wind Eng Ind Aerod 1997;67-68:459–77.
[24] Ng E, Yuan C, Chen L, Ren C, Fung JCH. Improving the wind environment in high-density cities by understanding urban morphology and surface roughness: a study in Hong Kong. Landsc Urban Plann 2011;101(1):59–74.
[25] Blocken B, Carmeliet J, Stathopoulos T. CFD evaluation of wind speed conditions in passages between parallel buildings – effect of wall-function roughness modifications for the atmospheric boundary layer flow. J Wind Eng Ind Aerod 2007;95:941–62.
[26] Letzel OM, Krane M, Raasch S. High resolution urban large-eddy simulation studies from street canyon to neighbourhood scale. Atomos Environ 2008;42: 8770–84.
[27] Murakami S. Environmental design of outdoor climate based on CFD. Fluid Dyn Res 2006;38(2–3):108–26.
[28] Ferziger JH, Peric M. Computational method for fluid dynamics. 3rd ed. Berlin; Heidelberg; New York; Barcelona; Hong Kong; London; Milan; Paris; Tokyo: Springer; 2002.
[29] Meneveau C, Katz J. Scale-invariance and turbulence models for large-eddy simulation. Annu Rev Fluid Mech 2000;32:1–32.
[30] Kleissl J, Parlange MB. Field experimental study of dynamic smagorinsky models in the atmospheric surface layer. J Atmos Sci 2004;61:2296–307.
[31] Kuznik F, Brau J, Rusaouen G. A RSM model for the prediction of heat and mass transfer in a ventilated room. Build Simulat; 2007:919–26.
[32] Wong FJ. Computational fluid dynamics analysis. Beijing, China: Tsinghua University Press; 2004.
[33] FLUENT 6.3 user's guide. Fluent Inc; 2006. 12–58.
[34] Menter FR, Kuntz M, Langtry R. Ten years of industrial experience with the SST turbulence model. Turbulence, Heat and Mass Transfer 2003;4:625–32.
[35] Mochida A, Tominaga Y, Murakam S, Yoshie R, Ishihara T, Ooka R. Comparison of various κ–ε models and DSM applied to flow around a high-rise building - Report on AIJ cooperative project for CFD prediction of wind environment. Wind Struct 2002;5(2–4):227–44.
[36] Kondo H, Asahi K, Tomizuka T, Suzuki M. Numerical analysis of diffusion around a suspended expressway by a multi-scale CFD model. Atomos Environ 2006;42(38):8770–84.
[37] Ashie Y, Hirano K, Kono T. Effects of sea breeze on thermal environment as a measure against Tokyo's urban heat island. The seventh international conference on urban climate. Japan: Yokohama; 2009.
[38] Wikipedia. Mong Kok. Available at: http://en.wikipedia.org/wiki/Mong_Kok; 2011.
[39] To AP, Lam KM. Evaluation of pedestrian-level wind environment around a row of tall buildings using a quartile-level wind speed descriptor. J Wind Eng Ind Aerod 1995;54–55:527–41.
[40] Yim SHL, Fung JCH, Lau AKH. Mesoscale simulation of year-to-year variation of wind power potential over southern China. Energies 2009;2:340–61.
[41] Cheng V, Ng E. Thermal comfort in urban open spaces for Hong Kong. Architect Sci Rev 2006;49(2):179–82.
[42] Murakami S, Deguchi K. New criteria for wind effects on pedestrians. J Wind Eng Ind Aerod 1981;7:289–309.
[43] Ng e, Cheng V, Chan C. Urban climatic map and standars for wind environment - feasibility study. Technical input report no. 1: methodologies and finds of user`s wind comfort level survey. Hong Kong Planning Department. Available at: http://www.pland.gov.hk/pland_en/p_study/prog_s/ucmapweb/ucmap_project/content/reports/Comfort_Level_Survey.pdf; 2008.
[44] Hoppe P. The physiological equivalent temperature - a universal index for the biometeorological assessment of the thermal environment. Int J Biometeorol 1999;43:71–5.
[45] Hong Kong planning standards and guidelines. Hong Kong planning Department; 2011 [Available at].
[46] Ng E. Towards a planning and practical understanding for the need of meteorological and climatic information for the design of high density cities - a case based study of Hong Kong. Int J Climatol; 2010. doi:10.1002/joc.2292.
[47] Mills G, Cleugh H, Emmanuel R, Endlicher W, Erell E, McGranahan G, et al. Climate information for improved planning and management of mega cities (needs perspective). Procedia Environ Sci 2010;1:228–46. doi:10.1016/j.proenv.2010.09.015.
[48] Waller J. Hong Kong the growth of the city. London, United Kingdom: Compendium Publishing; 2008.
[49] Moss P. Hong Kong an affair to remember. Hong Kong: From Asia Books Limited; 2008.
[50] Wolf M. Hong Kong outside. Hong Kong and Germany: Asia One Books and Peperoni Books; 2009.